VIII. RADIO ASTRONOMY

Academic and Research Staff

Prof. Alan H. Barrett
Prof. Bernard F. Burke
Prof. Philip C. Myers
Prof. David H. Staelin
Dr. José A. S. DeCampos
Dr. Alan Parrish
Dr. Philip W. Rosenkranz
John W. Barrett
John D. Kierstead
D. Cosmo Papa

Graduate Students

Manoug M. Ansourian
Patrick C. Crane
Arthur D. Fisher
Thomas S. Giuffrida
Aubrey D. Haschick
Paul T. Ho
James M. Johanson
Kai-Shue Lam
William H. Ledsham
Sylvester Lee
Robert N. Martin
Joseph W. Orenstein
Robert J. Parr
Ronald L. Pettyjohn
Matthew H. Schneps
Michael Shao
Robert C. Walker

1. MICROWAVE PROPAGATION IN THE TERRESTRIAL ATMOSPHERE

JSEP

Joint Services Electronics Program (Contract DAAB07-75-C-1346)

Alan H. Barrett

The propagation of microwave radiation through the terrestrial atmosphere has been investigated theoretically by using a theory that takes full account of the effects of overlapping spectral lines. At atmospheric pressures, lines of O_2 at $\lambda \approx 5$ mm and H_2O lines at submillimeter wavelengths overlap significantly, giving rise to line-to-line interference effects. Thus the absorption is not a straight summation of the absorption of individual lines. Self-broadening and foreign-gas broadening of O_2 and H_2O transitions in an atmospheric mix of O_2, N_2, and H_2O have been considered. The theory is in good agreement with experiment for the O_2 lines but fails to agree with H_2O absorption. Thus the long-standing problem remains of absorption in the far wings of many H_2O transitions at infrared frequencies. The discrepancy between theory and experiment for the H_2O absorption may be due to the inadequacy of the impact approximation that is used throughout, or to the existence of significant absorption caused by H_2O dimers. No further work on this project is planned during the coming year.

JSEP

2. MICROWAVE SPECTROSCOPY OF THE INTERSTELLAR MEDIUM

National Science Foundation (Grant AST73-05042-A02)

Alan H. Barrett, Philip C. Myers

During the past year our studies of the molecular components of the interstellar medium have continued with observations of microwave transitions of CO, CS, NH_3, HNCO, H_2CO, and CH_3OH. We have used radio telescopes at the Haystack Observatory, Tyngsboro, Massachusetts, the National Radio Astronomy Observatory, Green Bank, West Virginia, Kitt Peak Observatory, Arizona, and the Max Planck Institute, Bonn, West Germany. Observations of H and OH transitions will take place in January 1976, on the upgraded antenna at Arecibo, Puerto Rico. The greater part of our program is concerned with observing dense interstellar clouds, mapping the molecular distribution, and correlating the results with each other and with other properties of the clouds such as infrared observations made by others. Our results have shown that CS is a relatively common and abundant constituent of interstellar clouds and of the general interstellar medium along the galactic plane. Time variations of the CH_3OH maser emission from the KL nebula in Orion have been established and are the subject of further investigation. In collaboration with observers at the Berkeley observatory, we have mapped extensively NH_3 emission in Orion, and have also detected NH_3 in several clouds.

3. MICROWAVE THERMOGRAPHY

National Institutes of Health (Grant 5 SO5 RR07047-10)

Alan H. Barrett, Philip C. Myers

Our program of clinical evaluation of a microwave radiometer for purposes of breast cancer detection continues at Faulkner Hospital, in Boston, as part of the Sagoff Breast Cancer Detection Clinic. In analyzing our microwave maps, we found a high degree of variation in the measured temperatures. Much of the apparent variation has been traced to temperature variation of our reference loads and thermal conduction effects between antenna and patient tissue. We have installed a refrigerated chamber in our system to stabilize the temperature of the reference loads within ±0.1°C, and have constructed an insulated, temperature-controlled antenna housing to minimize conduction effects. The measured temperature variation with time has thereby been significantly reduced, and we may now place higher confidence in the measured spatial temperature patterns. These are now being compared with results of x-ray, infrared, and biopsy examinations in an attempt to determine an optimum cancer detection criterion for the microwave instrument. Preliminary results, based on a very small sample, indicate a microwave cancer detection rate comparable to that of the infrared technique.

In laboratory work we have concentrated on construction of a blanking circuit to permit operation of our 1.3 GHz system in environments with pulsed interference signals, application of a modulated-scattering technique to measure the near-field pattern of new antennas, and preparation for experiments to detect internal temperature increases associated with exercise.

4. ATMOSPHERIC MEASUREMENTS NEAR 118 GHz WITH PASSIVE MICROWAVE TECHNIQUES

U. S. Air Force – Electronic Systems Division (Contract F19628-75-C-0122)

David H. Staelin, Philip W. Rosenkranz

The use of the 118 GHz spectral region for sensing of atmospheric temperature profiles is being explored. A 118-GHz spectrometer is being built for studies of atmospheric opacity and cloud emission.

5. ASTROMETRIC INTERFEROMETER

M. I. T. Sloan Fund for Basic Research

David H. Staelin

A long-baseline Michelson interferometer is being developed for astrometric purposes. Relative stellar positions should be measured with $\sim 10^{-4}$-10^{-5} arc sec accuracy. Many astrophysical and geophysical experiments can be performed with such an instrument, including possible detection of planetary systems, relativistic deflection of starlight, and fluctuations in the local gravity gradient.

6. ENVIRONMENTAL SENSING WITH THE NIMBUS SATELLITE PASSIVE MICROWAVE SPECTROMETERS

National Aeronautics and Space Administration (Contract NAS5-21980)

David H. Staelin, Philip W. Rosenkranz

The Nimbus-5 and Nimbus-6 Earth observatory satellites were launched in December 1972 and June 1975. Each carried 5-channel microwave spectrometers operating in the water vapor and oxygen bands near 1-cm wavelength. The ability of the Nimbus-5 spectrometer to infer atmospheric temperature profiles at 0-20 km altitude in the presence of clouds has been documented[1,2] and has stimulated the inclusion of a 4-channel microwave spectrometer on the operational Tiros-N meteorological satellites, and a 7-channel unit on the corresponding Air Force satellites.

The Nimbus-6 spectrometer produces global maps of ~200 km resolution every 12 hours. These maps have revealed large systematic variations of snow in Antarctica that were unknown, and show interesting variations in tropical humidity. Parameter estimation theory is being applied to the interpretation of data.

a. Scanning Microwave Spectrometer on Nimbus-6

The Nimbus-6 Satellite was launched on June 11, 1975. It carries 9 experiments, most of which, including the Scanning Microwave Spectrometer (SCAMS), observe the Earth. SCAMS, which is a 5-channel microwave radiometer with mechanically scanning antennas,[3] is an improved version of the nadir viewing spectrometer on Nimbus-5.[4]

SCAMS has channels at 22.235, 31.65, 52.85, 53.85, and 55.45 GHz. The first two channels permit measurement of atmospheric water vapor and liquid water over ocean, and provide information about surface characteristics, such as snow and ice cover and soil moisture, over land. The three higher channels are used to retrieve the atmospheric temperature profile.

Preliminary data from orbit 47 over the intertropical convergence zone (ITCZ) in the Pacific Ocean are presented in Figs. VIII-1 and VIII-2. Figure VIII-1 shows contour maps of water vapor and liquid water, inferred from channels 1 and 2 by means of a statistical inversion method.[5] The maps were interpolated from the SCAMS scan pattern, which has 13 elements crosswise, and samples every 100 km parallel to the satellite track.[3] Figure VIII-2 is a longitudinal cut through the heaviest cloud region in Fig. VIII-1, i.e., at 0.45 Mm from the subpoint. Plotted in Fig. VIII-2 along with the water vapor and liquid water are uninverted (corrected only for sidelobes)

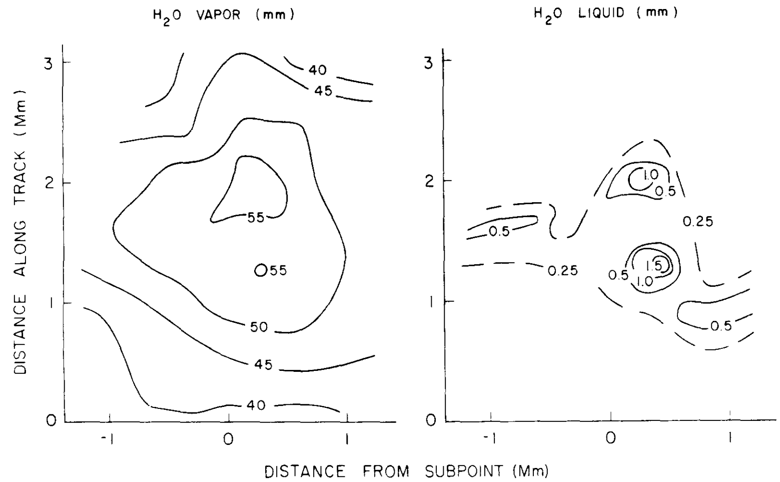

Fig. VIII-1. Contour maps of water vapor and liquid water retrieved from SCAMS data over the Pacific Ocean ITCZ, June 15, 1975.

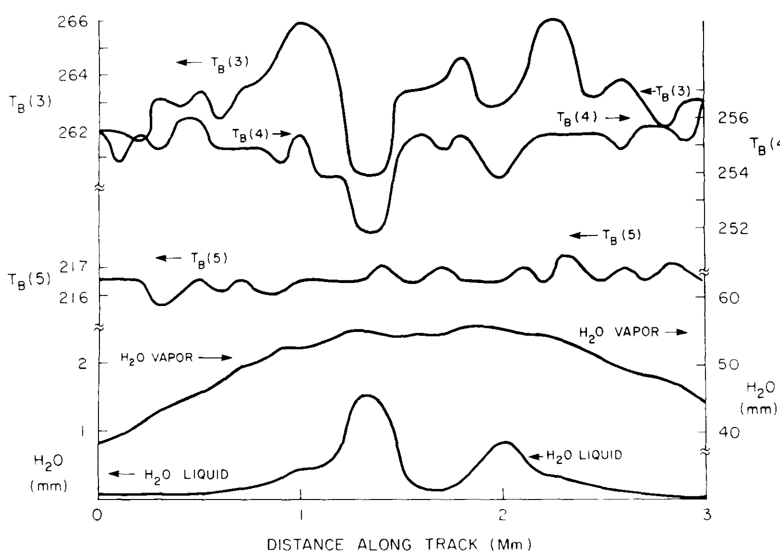

Fig. VIII-2. Longitudinal cut through the area shown in Fig. VIII-1 at 0.45 Mm from the subpoint.

brightness temperatures for the three higher frequency channels. Channels 3-5 are most sensitive to atmospheric temperature at altitudes near the surface, 5 km and 14 km, respectively (at this angle). Perturbations induced in the three temperature-sensing channels by clouds and water vapor can be seen. These perturbations are most severe in channel 3, weaker in channel 4, and negligible in channel 5. The ITCZ is the heaviest cloud situation normally encountered over the globe, so that over most areas cloud-induced effects on retrieved temperature profiles will be quite small.

References

1. D. H. Staelin, A. L. Cassel, K. F. Kunzi, R. L. Pettyjohn, R. K. L. Poon, P. W. Rosenkranz, and J. W. Waters, "Microwave Atmospheric Temperature Sounding: Effects of Clouds on the Nimbus-5 Satellite Data," J. Atmos. Sci. 32, 1970-1976 (1975).

2. J. W. Waters, K. F. Kunzi, R. L. Pettyjohn, R. K. L. Poon, and D. H. Staelin, "Remote Sensing of Atmospheric Temperature Profiles with the Nimbus-5 Microwave Spectrometer," J. Atmos. Sci. 32, 1953-1969 (1975).

3. D. H. Staelin, A. H. Barrett, P. W. Rosenkranz, F. T. Barath, E. J. Johnston, J. W. Waters, and A. Wouters, "The Scanning Microwave Spectrometer Experiment," in J. E. Sissala (Ed.), The Nimbus-6 Users Guide, February 1975, pp. 59-86.

4. D. H. Staelin, A. H. Barrett, J. W. Waters, F. T. Barath, E. J. Johnston, P. W. Rosenkranz, N. E. Gaut, and W. B. Lenoir, "Microwave Spectrometer on the Nimbus-5 Satellite: Meteorological and Geophysical Data," Science 182, 1339-1341 (1973).

5. J. W. Waters and D. H. Staelin, "Statistical Inversion of Radiometric Data," Quarterly Progress Report No. 89, Research Laboratory of Electronics, M. I. T., April 15, 1968, pp. 25-28.

7. FEASIBILITY STUDY OF A MICROWAVE SPECTROMETER FOR METEOROLOGICAL OBSERVATIONS FROM SYNCHRONOUS SATELLITES

National Aeronautics and Space Administration (Contract NAS5-22485)

David H. Staelin, Philip W. Rosenkranz

Continuous observations of the Earth by synchronous satellites are most useful if the spatial resolution is 50 km or better, which means that frequencies above 100 GHz are desirable. The use of this spectral region for determination of humidity and temperature is being explored.

A. ATMOSPHERIC OXYGEN AND WATER-VAPOR MICROWAVE ABSORPTION

JSEP

Joint Services Electronics Program (Contract DAAB07-75-C-1346)

Alan H. Barrett, Kai-Shue Lam

We present here results of calculations applied to atmospheric microwave absorption. The computational methods have been delineated in RLE Progress Reports No. 115 (pp. 74-83) and No. 116 (pp. 55-56).

With reference to an interaction potential for both O_2-O_2 and O_2-N_2 interactions of the form

$$V = \left(Ae^{-ar} - \frac{C}{r^6}\right) + P_2(\cos\theta)\left(Aa_r e^{-ar} - \frac{Ca_a}{r^6}\right),$$

we have used the following parameters for the O_2-N_2 case:

$A = 2.73 \times 10^5$ eV

$C = 42.2$ eV $\cdot$ Å^6

$a = 4.574\ \text{Å}^{-1}$

$a_r = 1.105$

$a_a = 0.229.$

With these parameters the ratio of the N_2 to O_2 broadening effectiveness is indicated to be ≈ 0.91.[1] The following formula is used to compute the absorption coefficient of dry air.

$$K_\nu(\text{Dry Air}) = \frac{0.61576\ P\nu^2}{T^3}(-1)\ \text{Im}\left[\underline{d}^T \cdot \left(\nu\underline{\underline{I}} - \underline{\underline{\nu}}_o - 10^{-3}\ P\sum_i x_i\underline{\underline{\gamma}}_i\right)^{-1} \cdot \underline{\underline{\rho}}''^r \cdot \underline{d}\right]\ \text{N/km}$$

where

P = pressure (Torr)

T = temperature (°K)

ν = observation frequency (GHz)

$\underline{\underline{\nu}}_o$ = resonance frequency matrix (GHz)

$\underline{d}$ = reduced dipole moment matrix for O_2 (dimensionless)

$\underline{\underline{\gamma}}_i$ = interaction matrix (O_2-O_2 or O_2-N_2) (MHz/Torr)

$\underline{\underline{\rho}}''^r = 0.725\ T\underline{\underline{\rho}}^r$ with

$\underline{\underline{\rho}}^r$ = population matrix for O_2.

JSEP

JSEP

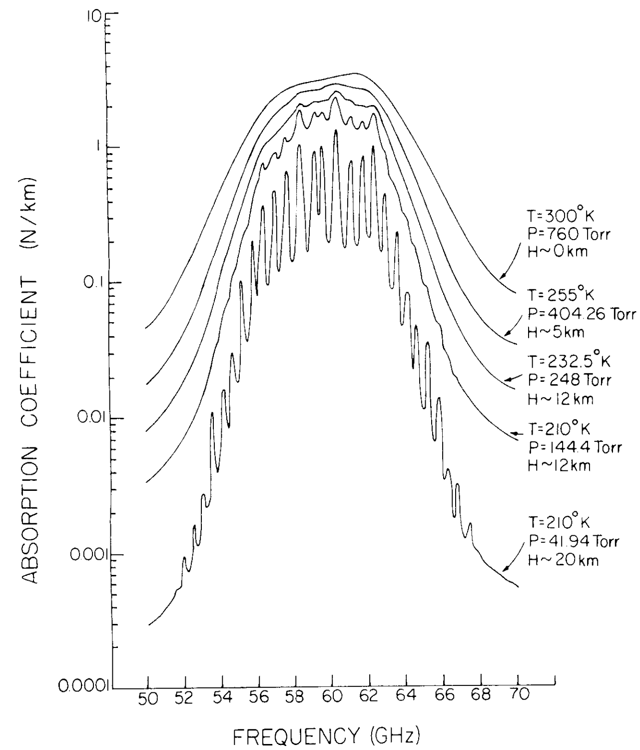

Fig. VIII-3.

Computed dry air absorption coefficients.

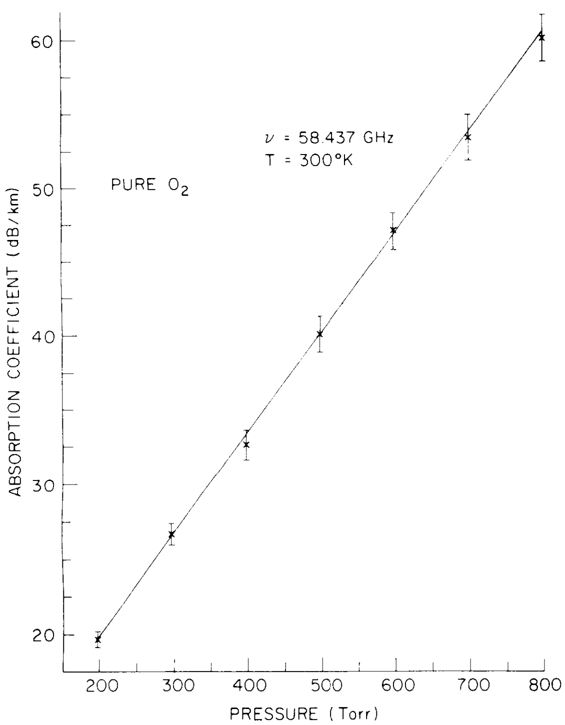

Fig. VIII-4.

Computed and measured pure oxygen absorption coefficient pressure profile. Experimental results from Liebe.[2]

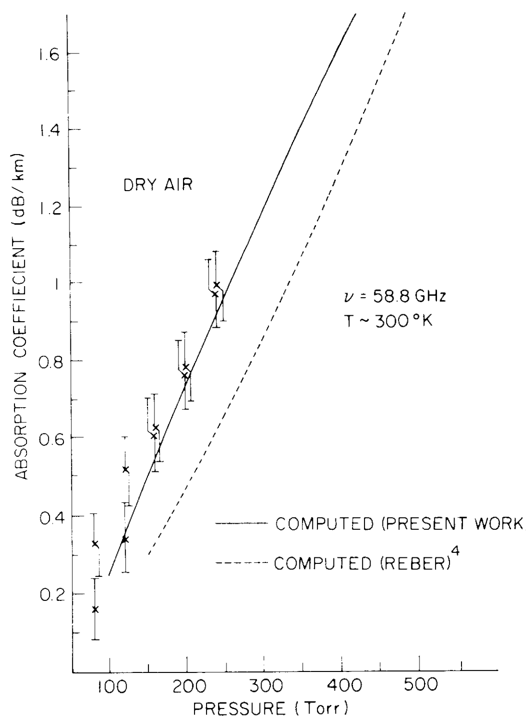

Fig. VIII-5.

Computed and measured dry air absorption coefficient vs pressure profiles. Experimental results from Poon.[3]

JSEP

JSEP

The summation index i is over the two perturbers O_2 and N_2, with

$$X_{O_2} = \text{fractional partial pressure of } O_2 = 0.21$$

$$X_{N_2} = \text{fractional partial pressure of } N_2 = 0.78.$$

Figure VIII-3 shows computed results for K_ν (Dry Air) for atmospheric conditions from ground level to the lower layers of the tropopause. Figures VIII-4 and VIII-5 give a comparison between computed absorption coefficient pressure profiles and experimental results for pure O_2 and dry air at selected frequencies. Pressure broadening theory indicates that line overlapping results from nonvanishing of the off-diagonal interaction matrix elements. This effect is illustrated for dry air absorption at T = 300°K and

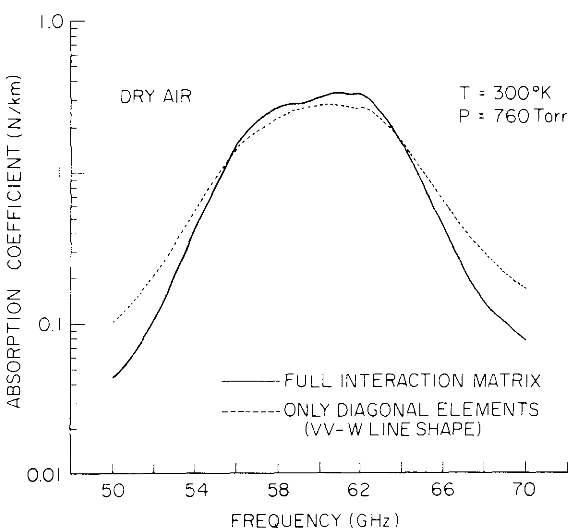

Fig. VIII-6.

Theoretical demonstration of overlapping effects for O_2 microwave absorption. Absorption coefficients are computed for dry air.

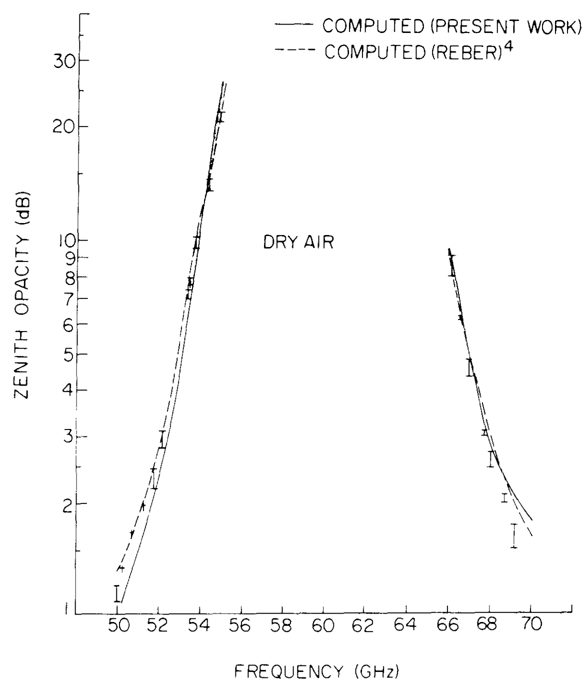

Fig. VIII-7.

Computed and measured zenith opacities (dry air). Overview of the oxygen band. Experimental results from Reber.[4]

P = 760 Torr (ground level) in Fig. VIII-6, which shows the collapse of the overlapping band shape as compared with the noninterfering band shape. Figure VIII-7 gives a comparison between computed and measured zenith opacities.

JSEP

Table VIII-1. Computed and selected experimental results for dipole-quadrupole linewidths for eleven H_2O resonant lines.

Line	Resonant Frequency (GHz)	Linewidth (MHz/Torr) O_2 Broadened		N_2 Broadened		T = 300°K Dry Air Broadened	
		Computed	Experimental	Computed	Experimental	Computed	Experimental
1_{01} 1_{10}	556.936	2.686		4.143		3.798	
2_{02} 2_{11}	752.033	2.653		4.092		3.749	
2_{20} 3_{13}	183.310	2.657	2.72 ± .03 [1]	4.098	3.76 ± .05 [1]	3.754	
			2.70 [2]		4.40 [2]		
					4.2 ± .6 [4]		
3_{21} 4_{14}	380.197	2.693		4.155		3.806	3.75 ±.28 [3]
3_{30} 4_{23}	448.001	2.687		4.144		3.797	
4_{22} 5_{15}	325.153	2.725		4.203		3.851	
4_{40} 5_{33}	474.689	2.741		4.227		3.873	
4_{41} 5_{32}	620.701	2.627		4.052		3.712	
5_{23} 6_{16}	22.235	2.739	2.52 [5]	4.226	4.10 [5]	3.773	3.43 ±. 39 [6]
5_{50} 6_{43}	439.151	2.686		4.143		3.796	
5_{51} 6_{42}	470.889	2.698		4.161		3.812	

References: [1] Rusk,[5] [2] Frenkel and Woods,[6] [3] Pearson et al.,[7] [4] Emery,[8] [5] Liebe and Dillon,[9] [6] Becker and Autler.[10]

JSEP

Only dipole-quadrupole interactions (H_2O-O_2 and H_2O-N_2) have been considered for the H_2O absorption. The interaction matrix element is written

$$\frac{\gamma_{ij}^{d-q}}{P} = 1.78 \times 10^{28} \frac{(\mu, Q_2)^{2/3}}{T^{5/6} m_r^{1/6}} \delta_{ij}^{d-q} \text{ MHz/Torr},$$

where P = pressure (Torr), T = temperature (°K), μ_1, Q_2 = dipole and quadrupole moments of absorber and perturber (ESU), m_r = reduced mass of H_2O perturber two-molecule system (g), and δ_{ij}^{d-q} is a quantity that is only dependent on the quantum numbers of the rotational states involved in the interacting lines. The linewidths are just given by γ_{ii}^{d-q}/P. In Table VIII-1 a comparison of computed and experimental linewidths for 11 lines is presented. These computations have been made using the following choice of parameters:

$$\mu_{H_2O} = 1.884 \times 10^{-18} \text{ ESU}$$

$$Q_{O_2} = 0.82 \times 10^{-26} \text{ ESU}$$

$$Q_{N_2} = 1.55 \times 10^{-26} \text{ ESU.}$$

Since the amount of computation for lines with high rotation quantum numbers is prohibitive, the matrix $\underline{\underline{\delta}}$ have been computed explicitly for only 9 lines (resonance frequency less than 800 GHz and lower energy state of the transition pair with energy less than 500 cm^{-1}). Some conclusions can be drawn, however, about the importance of the overlapping effects from the general properties of the matrix elements derivable from this submatrix. Using hypothetical values for δ_{ij}, we have computed absorption spectra for an interaction matrix covering 17 lines (lower energy state less than 1400 cm^{-1}). Our estimative conclusion is that the overlapping effects, which contribute ~5% at most, are inadequate to account for the anomalous H_2O absorption in the microwave region which was unexplained previously.

References

1. H. J. Liebe, Office of Telecommunications Report 75-00, U.S. Department of Commerce, Washington, D.C., 1975.
2. H. J. Liebe, Office of Telecommunications Report 75-65, U.S. Department of Commerce, Washington, D.C., 1975.
3. R. K. L. Poon, Sc.D. Thesis, M.I.T., 1974.
4. E. E. Reber, J. Geophys. Res. 77, 3831 (1972).
5. J. R. Rusk, J. Chem. Phys. 42, 493 (1965).
6. L. Frenkel and D. Woods, Proc. IEEE 54, 498-505 (1966).
7. J. E. Pearson, D. T. Llewellyn-Jones, and R. J. Knight, Infrared Phys. 9, 53-58 (1969).
8. R. Emery, Infrared Phys. 12, 65 (1972).
9. H. J. Liebe and T. A. Dillon, J. Chem. Phys. 50, 727-732 (1969).
10. G. E. Becker and S. H. Autler, Phys. Rev. 70, 300-307 (1946).

JSEP